INTERNATIONAL JOURNAL FOR NUMERICAL METHODS IN FLUIDS
Int. J. Numer. Meth. Fluids 2003; **41**:675–694 (DOI: 10.1002/fld.461)

Development of highly accurate interpolation method for mesh-free flow simulations III. Analysis of accuracy and stability

Nobuatsu Tanaka*,†

Department of Mechanical Engineering, Ibaraki University 4-12-1, Naka-Narusawa, Hitachi, Ibaraki 316-8511, Japan

SUMMARY

A highly accurate interpolation method, CIVA, improves the accuracy of mesh-free and grid-less methods by taking into consideration first-order spatial derivatives as variables; an approach based on the same idea as that on which CIP is based. In this study, the accuracy and stability of CIVA is evaluated by analytically and numerically. First, the general formulation of CIVA for the n-dimensional case is described. Since CIVA contains the bubble function, we consider the determination methods: constant curvature condition and utilization of another computing point. Then, the relation between the bubble function in the CIVA method and the accuracy and stability is made clear by the analysis based on the Taylor expansion. Some computations of two-dimensional passive scalar advection and advection–diffusion problems are performed for the verification of accuracy and stability. Copyright © 2003 John Wiley & Sons, Ltd.

KEY WORDS: CIVA; accuracy; stability; bubble function; n-simplex

1. INTRODUCTION

In the field of computational fluid dynamics (CFD), numerical accuracy and stability are the most important factors because they can have fatal effects on the results. However, it is difficult to be consistent with regard to these two factors. Accordingly, researchers have developed several kinds of consistent methods, for example, the high-order schemes (e.g. UTOPIA and K-K) in finite difference method (FDM) and high-order elements in finite element method (FEM). However, these methods are mesh-based and are not applicable to mesh-free approaches. Mesh-free approaches have been attracting the attention of researchers in the field of the fluid dynamics because they do not require mesh generation, which generally is time-consuming and requires great care. The particle-in-cell method [1], gridless method [2], SPH

* Correspondence to: N. Tanaka, Department of Mechanical Engineering, Ibaraki University, 4-12-1 Naka Narusawa, Hitachi, Ibaraki 316-8511, Japan.
† E-mail: tanaka@mech.ibaraki.ac.jp

Received September 2001
Revised 26 August 2002

[3], RKPM [4] and NEM [5], are popular in CFD, but have drawbacks in that improvement of numerical accuracy and application to high Reynolds number flow are difficult. In mesh-free methods, the interpolation method is so important as to determine the computational accuracy. In the conventional mesh-free method, the numerical viscosity produced by the interpolation (or function approximation) becomes a serious problem, because there is no highly accurate interpolation algorithm applicable to mesh-free techniques. We therefore propose a highly accurate interpolation method for mesh-free techniques. In mesh-free methods, interpolation of value at a target point is performed using the data of points around the position. Use of the least-squares method causes numerical error in the approximation of functions. Therefore, the increase of points and the use of higher-order function do not necessarily lead to improvement of accuracy. That is, interpolation should generally be performed using as few points as possible. Such points in nth dimensions form n-simplex, and these forms are suitable from the viewpoint of flexibility because we only locally compose a suitable n-simplex (local mesh) including the target point for interpolation from calculation points when interpolation is required.

Therefore, we have developed a new highly accurate and stable interpolation algorithm applicable to mesh-free methods [6]. To achieve high accuracy and stability, we improve the cubic-interpolated pseudo-particle (CIP) method [7, 8], which in its original form executes interpolation with a rectangle or rectangular parallelepipeds mesh, for n-simplex (where n means the dimensions of Euclidian space) and barycentric co-ordinates. Barycentric co-ordinates are popularly called the volume co-ordinates in three dimensions and the area co-ordinates in two dimensions. The new interpolation method, which we call cubic interpolation with volume/area co-ordinates (CIVA), makes it possible to achieve highly accurate interpolation based on n-simplex in the case of mesh-free methods. The similar idea, called natural element method (NEM), was recently presented by Sukumar *et al*. [5]. While the NEM interpolation is based upon a local n-simplex, the higher-order interpolation by NEM also requires some pieces of n-simplexes (a lot of computing points), similarly to the other foregoing meshless method. The CIVA method, however, requires only one n-simplex for third-order interpolation by introducing the idea of CIP method. This is the great advantage of CIVA over the other meshless methods. In this paper, we briefly describe the CIVA method and evaluation of the accuracy and stability by mathematical and numerical analyses.

2. CIVA METHOD

To formulate the CIVA method, it is necessary to work with piecewise polynomial functions defined on n-simplexes. For that purpose, we recall here the underlying definitions and notations of n-simplexes and barycentric co-ordinates.

2.1. Barycentric co-ordinates and n-simplex

Let $P_1, \ldots, P_{n+1}$ be points geometrically independent in $\mathbf{R}^n$, that is, no $(n-1)$-dimensional hyperplane contains all the $n+1$ points. Then, the n vectors $P_2P_1, P_3P_1, \ldots, P_{n+1}P_1$ are

independent, which means

$$\mathbf{A}=\begin{pmatrix}\mathbf{p}_1 & \mathbf{p}_2 & \cdots & \mathbf{p}_{n+1}\\ 1 & 1 & \cdots & 1\end{pmatrix}=\begin{pmatrix}x_{1,1} & x_{2,1} & \cdots & x_{n+1,1}\\ \vdots & & & \vdots\\ x_{1,n} & x_{2,n} & \cdots & x_{n+1,n}\\ 1 & 1 & \cdots & 1\end{pmatrix} \tag{1}$$

is non-singular, where the co-ordinates of P_i $(1\leqslant i\leqslant n+1)$ are $\mathbf{p}_i=OP_i=(x_{i,1},\ldots,x_{i,n})^{\mathrm{t}}$ and O is the origin of $\mathbf{R}^n$. Given any point $Q\in\mathbf{R}^n$, with co-ordinates $\mathbf{x}=(x_1,\ldots,x_n)^{\mathrm{t}}$, there exist $(n+1)$ real numbers

$$\lambda_i=\lambda_i(\mathbf{x}),\quad 1\leqslant i\leqslant n+1 \tag{2}$$

such that

$$\mathbf{x}=\sum_{i=1}^{n+1}\lambda_i\mathbf{p}_i,\quad \sum_{i=1}^{n+1}\lambda_i=1 \tag{3}$$

It is clear that Equations (3) are equivalent to the linear system

$$\mathbf{A}\begin{pmatrix}\lambda_1\\ \vdots\\ \lambda_n\\ \lambda_{n+1}\end{pmatrix}=\begin{pmatrix}x_1\\ \vdots\\ x_n\\ 1\end{pmatrix} \tag{4}$$

which has a unique solution, since the matrix $\mathbf{A}$ is non-singular. The quantities λ_i are called the barycentric co-ordinates of Q, with respect to the $(n+1)$ points $P_1,P_2,\ldots,P_{n+1}$. As a consequence of Equation (4), the numbers λ_i appear as a linear function of the co-ordinates $x_1,\ldots,x_n$ of Q:

$$\lambda_i=\sum_{j=1}^{n}\frac{(\mathbf{A}^a)_{i,j}}{\det\mathbf{A}}x_j+\frac{(\mathbf{A}^a)_{i,n+1}}{\det\mathbf{A}},\quad 1\leqslant i\leqslant n+1 \tag{5}$$

where $\det\mathbf{A}$ is the determinant of $\mathbf{A}$ and $(\mathbf{A}^a)_{i,j}$ is the (i,j)-element of the adjugate matrix of $\mathbf{A}$. From this equation, we can obtain a differential property of the λ_i considered as functions of the Cartesian co-ordinates $x_1,\ldots,x_n$, of Q.

$$\frac{\partial}{\partial x_i}=\sum_{j=1}^{n+1}\frac{(\mathbf{A}^a)_{j,i}}{\det\mathbf{A}}\frac{\partial}{\partial\lambda_j},\quad 1\leqslant i\leqslant n \tag{6}$$

It is easy to see that the barycentric co-ordinates are independent of the choice of the basis in $\mathbf{R}^n$. The convex cell of the $(n+1)$ points P_i is exactly the set of points of $\mathbf{R}^n$ with barycentric co-ordinates satisfying the conditions:

$$0\leqslant\lambda_i\leqslant 1,\quad 1\leqslant i\leqslant n+1 \tag{7}$$

These conditions are also useful to efficiently judge whether an n-simplex contains a point or not in a program code. This convex cell $\langle P_1\ldots P_{n+1}\rangle$ is the n-simplex generated by the points P_i, which are called the vertices of the n-simplex. The barycentre G of the n-simplex is the point whose barycentric co-ordinates are all equal to $1/(n+1)$.

2.2. Formulation of CIVA

In this section, we consider the concrete formulation of CIVA. The objective of the CIVA method is to interpolate the value at a point in an n-simplex by a polynomial of degree three. Similar to the CIP method, we suppose that the scalar value and the spatial derivatives are given at every computing point (vertex of the n-simplex).

2.2.1. One-dimensional case.

In the one-dimensional case, the CIVA method without bubble functions is the same as the CIP method. The difference lies in the formulation. Here, as an introduction to CIVA, we will briefly explain the one-dimensional formulation of the CIVA method. Upon consideration of the one-, two- and three-dimensional cases, the consistency (universality) of the CIVA formulation in any dimension will become apparent.

One-dimensional simplex (1-simplex) $\langle P_1P_2\rangle$ is a segment or a line, and the barycentric co-ordinates of a point (λ_1, λ_2) represent the ratio of the distance from the segment edges to the segment length. The third-order polynomial by way of barycentric co-ordinates is expressed as

$$(\lambda^* f)(x) = \sum_{i=1}^{2} \alpha_i \lambda_i(x) + d \sum_{j,k=1(j\neq k)}^{2} \beta_{jk} \lambda_j^2(x) \lambda_k(x) \tag{8}$$

where $\lambda^* f$ is the pull-back under λ of the function f and the parameter d is the regulation parameter from the first-order to the third-order interpolation, and serves as the third-order interpolation in the case of $d=1$ and the first-order interpolation in the case of $d=0$. We use $d=1$ in this study except for the stabilizing method by controlling d-parameter in Section 2.2. By using relation (6), the coefficients α_i and β_{jk} are determined with the Cartesian co-ordinate values x_1, x_2, the scalar values f_1, f_2, and the spatial derivatives f_1', f_2' by

$$\alpha_i = f_i, \quad \beta_{jk} = f_j - f_k + (x_k - x_j) f_j' \tag{9}$$

By substituting $x_1 = 0$ and $x_2 = \Delta x$ ($x = x - x_1$), which means $\lambda_1 = (\Delta x - x)/\Delta x$ and $\lambda_2 = x/\Delta x$ from Equation (1), into Equations (8) and (9), we obtain the same formulation as in the case of the one-dimensional CIP [7]

$$f(x) = ax^3 + bx^2 + f_1' x + f_1 \tag{10}$$

where

$$a = \frac{1}{\Delta x^2}(f_1' + f_2') + \frac{2}{\Delta x^3}(f_1 - f_2), \quad b = -\frac{1}{\Delta x}(2f_1' + f_2') - \frac{3}{\Delta x^2}(f_1 - f_2) \tag{11}$$

2.2.2. Two-dimensional case.

The two-dimensional complete cubic polynomial with Cartesian co-ordinates, $\mathbf{x} = (x_1, x_2)$, is defined as

$$f(x) = \sum_{i,j=0(i+j\leqslant 3)}^{3} a_{ij} x_1^i x_2^j \tag{12}$$

When we try to use the cubic polynomial to interpolate within a 2-simplex (triangle) $\langle P_1P_2P_3\rangle$ in the same way as in the case of the CIP method, there are only 9 known pieces of

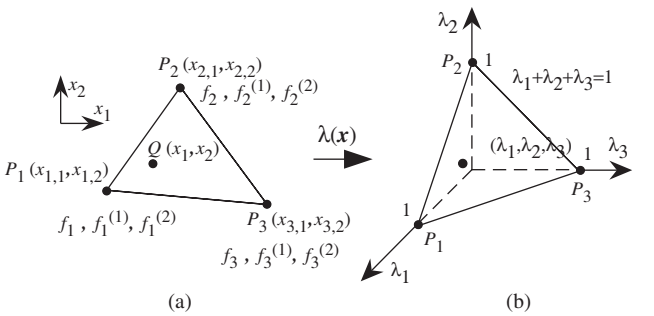

Figure 1. *n*-simplex and barycentric co-ordinates in two dimensions. (a) 2-simplex in cartesian co-ordinates; (b) Normalization by area co-ordinates.

information for the 10 unknown coefficients of Equation (12). Thus, the available information is insufficient. We solve the problem by reducing the unknown coefficients. If we reduce the unknown coefficients of Equation (12) in Cartesian co-ordinates, the following problems generally arise.

(A) The symmetric property of the function collapses.
(B) Simultaneous linear equations of coefficients have to be solved. This requires a long calculation time.
(C) The equations become singular if the triangle takes a certain form.

These problems can be solved by using the barycentric co-ordinates such as area co-ordinates and volume co-ordinates that are commonly used in the FEM field. Figure 1 shows the relation between Cartesian co-ordinates and barycentric co-ordinates in two dimensions.

Here, to maintain symmetry, the cubic function corresponding to the scalar quantity in a triangle is set in the following form via the area co-ordinates $(\lambda_1, \lambda_2, \lambda_3)$:

$$(\lambda^* f)(\mathbf{x}) = \sum_{i=1}^{3} \alpha_i \lambda_i(\mathbf{x}) + d \sum_{j,k=1(j\neq k)}^{3} \beta_{jk}[\lambda_j^2(\mathbf{x})\lambda_k(\mathbf{x}) + b_{jk}^{\{2\}}(\mathbf{x})] \tag{13}$$

where $b_{jk}^{\{2\}}(\mathbf{x})$ is a set of the functions with support restricted to the triangle. The function is similar to the bubble function in FEM [9, 10], and so we call it the bubble function. First we must provide a method to determine the bubble function, because the first-order spatial differential values become zero at every vertex of a triangle; therefore, the bubble function cannot be completely determined from the known information of the vertices. This is the reason for the singularity described above. This setting up of the bubble function is explained in the next section in detail. On the other hand, the remaining 9 unknown coefficients of Equation (13) can be determined independently of the bubble function and directly without solving simultaneous linear equations. We define $f_h^{\overbrace{(i,j,\ldots,k)}^{m}}$ as $(\partial^m f/\partial x_i \partial x_j \cdots \partial x_k)|_{P_h}$. Using the relations of the two-dimensional partial-differential operators in (6), we can simply determine the

unknown coefficients to be

$$\alpha_i = f_i, \quad \beta_{jk} = f_j - f_k + \sum_{l=1}^{2} (x_{k,l} - x_{j,l}) f_j^{(l)} \tag{14}$$

where $x_{i,j}$ is the jth co-ordinate value of the ith point. Therefore, if the concrete form of the bubble function is given, we can interpolate the scalar quantities in a triangle from the set of Equations (13) and (14). The derivatives can also be interpolated by using Equations (6).

2.2.3. Three-dimensional case.
In the case of three dimensions, the CIVA method utilizes a tetrahedron (3-simplex) $\langle P_1 P_2 P_3 P_4 \rangle$ for interpolation and the volume co-ordinates (the three-dimensional barycentric co-ordinates). The following three-dimensional cubic polynomial using volume co-ordinates $(\lambda_1, \lambda_2, \lambda_3, \lambda_4)$ in a tetrahedron can be assumed as an example.

$$(\lambda^* f)(\mathbf{x}) = \sum_{i=1}^{4} \alpha_i \lambda_i(\mathbf{x}) + d \sum_{j,k=1(j\neq k)}^{4} \beta_{jk} [\lambda_j^2(\mathbf{x}) \lambda_k(\mathbf{x}) + b_{jk}^{\{3\}}(\mathbf{x})] \tag{15}$$

where $b_{jk}^{\{3\}}(\lambda)$ is a bubble function. Without solving the linear system, the coefficients α_i and $\beta_{j,k}$ can be calculated independently of the bubble function as follows:

$$\alpha_i = f_i, \quad \beta_{jk} = f_j - f_k + \sum_{l=1}^{3} (x_{k,l} - x_{j,l}) f_j^{(l)} \tag{16}$$

2.2.4. n-dimensional case.
From the above discussion, we can confirm that the barycentric co-ordinates make it possible to solve problems (A)–(C) in Section 1.2.2 and enable the cubic interpolation of the scalar distribution in an n-simplex using a simple and consistent formulation irrespective of dimension.

Summarizing this section, we can conclude that the n-dimensional ($n \geqslant 1$) CIVA interpolation function in n-simplex $\langle P_1 \cdots P_{n+1} \rangle$ is described by

$$(\lambda^* f)(\mathbf{x}) = \sum_{i=1}^{n+1} \alpha_i \lambda_i(\mathbf{x}) + d \sum_{j,k=1(j\neq k)}^{n+1} \beta_{jk} [\lambda_j^2(\mathbf{x}) \lambda_k(\mathbf{x}) + b_{jk}^{\{n\}}(\lambda(\mathbf{x}))]$$

$$\alpha_i = f_i, \quad \beta_{jk} = f_j - f_k + \sum_{l=1}^{n} (x_{k,l} - x_{j,l}) f_j^{(l)} \tag{17}$$

where $b_{jk}^{\{n\}}(\lambda)$ is a suitable n-dimensional bubble function.

2.3. Determination of the bubble functions

Since the support of bubble functions is restricted to the n-simplex, the functions do not influence the scalar values and the derivatives at the vertices of the n-simplex. Therefore, we must provide the way to determine the functions. In this part, we will consider two methods to determine the bubble functions in two and three dimensions.

2.3.1. Constant curvature condition

2.3.1.1. Two dimensions. As an example of the two-dimensional case, we consider a widely used bubble function with area co-ordinates,

$$b_{jk}^{\{2\}}(\lambda)=c\lambda_1\lambda_2\lambda_3 \tag{18}$$

where c is the control parameter, and a method of determining its value must be provided in advance. For example, we can use $c=\frac{1}{2}$. This value is chosen so that the cubic function expressed by Equation (13) gives arbitrary gradient in all the areas within a triangle. This is the constant curvature condition [11, 12]. In this sense, *curvature* in the constant curvature condition means *gradient*. The condition implies that the parameter c should be determined to satisfy

$$S_3^c \supset S_2 \tag{19}$$

where S_3^c is the function space spanned by the (incomplete) cubic polynomial of (13) with (14) and (18) is the function space spanned by the complete second-order polynomial, which can be expressed using area co-ordinates by

$$g(\lambda_1,\lambda_2,\lambda_3)=\sum_{i=1}^{3} p_i\lambda_i+\sum_{j,k=1(k>j)}^{3} q_{jk}\lambda_j\lambda_k \tag{20}$$

To equalize the scalar and derivative values of f and those of g at the triangle vertices, the following relations are established:

$$\alpha_i = p_i, \quad 1\leqslant i\leqslant 3 \tag{21}$$

$$\left.\frac{\partial f}{\partial x_i}\right|_{P_j} = \left.\frac{\partial g}{\partial x_i}\right|_{P_j}, \quad 1\leqslant j\leqslant 3, 1\leqslant i\leqslant 2 \tag{22}$$

Substituting relations (21) and the results obtained by relation (22) into Equation (13), and rearrangement by p_i and q_{jk} causes

$$\begin{aligned} f(\lambda_1,\lambda_2,\lambda_3)=&\sum_{i=1}^{3} p_i\lambda_i+q_{12}\lambda_1\lambda_2(\lambda_1+\lambda_2+2c\lambda_3\\ &+q_{23}\lambda_2\lambda_3(2c\lambda_1+\lambda_2+\lambda_3)+q_{13}\lambda_1\lambda_3(\lambda_1+2c\lambda_2+\lambda_3) \end{aligned} \tag{23}$$

By comparing Equations (23) and (20) and taking into account of the characteristic of barycentric co-ordinates, Equation (3), we can find that if and only if c is equal to $1/2$, the cubic polynomial (13) recovers the complete second-order polynomial and satisfies the constant curvature condition.

2.3.1.2. Three dimensions. For an example in the case of three dimensions, the following bubble function using volume co-ordinates $(\lambda_1,\lambda_2,\lambda_3,\lambda_4)$ in a tetrahedron, whose function is in more general form than that of the previous paper [6], is assumed in this study.

$$b_{jk}^{\{3\}}(\lambda)=\sum_{l=1}^{4} c_l\frac{\lambda_1\lambda_2\lambda_3\lambda_4}{\lambda_l} \tag{24}$$

where the parameter c_l is the control parameter, whose value we have to specify in advance. The reason is that the terms of $\lambda_1\lambda_2\lambda_3\lambda_4/\lambda_l$ $(l=1,2,3,4)$ and the first-order spatial differential values become zero at every vertex of the tetrahedron and their coefficients cannot be determined from the known information respecting the vertices. The constant curvature conditions can be also useful to determine the parameters c_l. By the same treatment as in two dimensions, it is possible to reduce the four parameters c_l of (24) into one parameter c by

$$b_{jk}^{\{3\}}(\lambda)=c\lambda_j\lambda_k(1-\lambda_j-\lambda_k) \tag{25}$$

The following is necessary to satisfy constant curvature conditions

$$c=\frac{1}{2} \tag{26}$$

The parameter c in Equation (25) can be expected to play the same role as that in two dimensions and be able to control the stability of the solution. The final form of the three-dimensional interpolating function with the constant curvature conditions becomes

$$(\lambda^* f)(\mathbf{x})=\sum_{i=1}^{4}\alpha_i\lambda_i(\mathbf{x})+\frac{1}{2}\sum_{j,k=1(j\neq k)}^{4}\beta_{jk}\lambda_j(\mathbf{x})\lambda_k(\mathbf{x})[1+\lambda_k(\mathbf{x})-\lambda_j(\mathbf{x})] \tag{27}$$

Therefore, by using the constant curvature condition, a scalar value and the spatial derivatives in a tetrahedron can be interpolated with the only known information (the Cartesian co-ordinate values, the scalar values and the spatial derivatives) respecting the vertices from Equations (16) and (27).

2.4. Accuracy and stability estimation

2.4.1. Problem considered and the governing equations.

Here, we analyse accuracy and stability of the CIVA-based method with a simple but important problem of passive scalar advection. The governing equation for passive scalar advection of scalar $\hat{f}$ by a flow $u=(u_1,u_2,\ldots,u_n)$ is

$$\frac{\partial\hat{f}}{\partial t}+u_i\frac{\partial\hat{f}}{\partial x_i}=0 \tag{28}$$

where repeated indices are summed. Sufficiently smooth function $\hat{f}$ represents the exact solution of Equation (28) in comparison with the approximated solution f. A feature of the CIP method is the achievement of third-order interpolation using the spatial derivatives as variables by considering the advection of not only the scalar quantity but also its derivatives. Therefore, the supplementary equations for the spatial derivatives are

$$\frac{\partial\hat{f}^{(j)}}{\partial t}+u_i\frac{\partial\hat{f}^{(j)}}{\partial x_i}=-\frac{\partial u_i}{\partial x_j}\frac{\partial\hat{f}}{\partial x_i},\quad j=1,2,\ldots,n \tag{29}$$

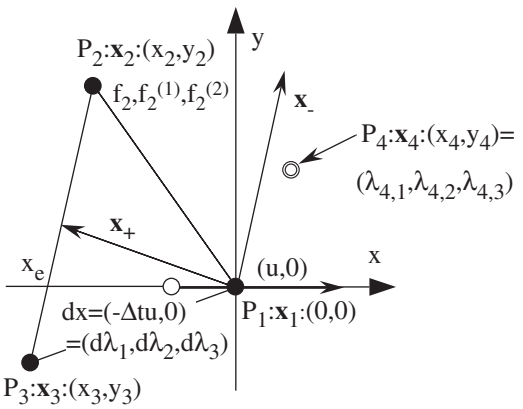

Figure 2. Co-ordinate system.

2.4.2. Accuracy and stability estimation based on Taylor expansion.
In the two-dimensional case, the scalar distribution $\hat{f}$ at t^n is approximated by function (13) with the bubble function (18) by

$$f^n = \sum_{i=1}^{3} \alpha_i \lambda_i + \sum_{j,k=1(j\neq k)}^{3} \beta_{jk} \lambda_j^2 \lambda_k + c' \lambda_1 \lambda_2 \lambda_3 \tag{30}$$

where $c' = c\Sigma\beta_{jk}$. The last term of Equation (30) is the same as the bubble function of the finite element method. It turns out that the FEM using bubble functions can improve stability by the same effect of artificial viscosity as in the case of using the SUPG method [9, 10].

Therefore, we can consider that the term is related with the accuracy and stability of the CIVA method. Here, the meanings of the bubble function in the CIVA method are considered based on the Taylor expansion analysis. The target point for consideration is P_1 and the point is supposed to be the origin of reference co-ordinates. The points P_1, P_2 and P_3 compose a triangle used for interpolation and P_2 and P_3 are in the second and third quadrant (Figure 2), respectively. We suppose a uniform flow in the direction of x_1, $\mathbf{u} = (u, 0)$, in order to simply analyse accuracy and stability. In this case, we can regard the CIVA-particle method that initializes the particle location every time step and the CIVA-gridless method as the same approach.

The CIVA-particle method is a highly accurate Lagrangian method where an observer analyses the fluid behaviour around him as he moves with a fluid particle, which transfers not only the physical quantities but also the spatial derivative values. Therefore, we can perform the high-order interpolation, CIVA, and flexibly rearrange the particle positions. Meanwhile, the CIVA-gridless method is a highly accurate Eulerian method that updates the fluid field around a fixed geometrical point every time-step by utilizing the upwind technique. The upwind technique computes the physical value at a target point and the next time-step by interpolating the value at the upwind position of a target point. In order to reduce the numerical error, the CIVA-gridless method utilizes the CIVA method for the interpolation [6, 7]. Both

the methods approximate the value at P_1 and at the next time step t^{n+1} by

$$f_1^{n+1} = f^n(\mathrm{d}\mathbf{x}) = f^n(\mathrm{d}\lambda_1, \mathrm{d}\lambda_2, \mathrm{d}\lambda_3)(\cong \hat{f}|_{t^{n+1}, P_1}) \tag{31}$$

where $\mathrm{d}\mathbf{x} = -\Delta t\mathbf{u}$ in Cartesian co-ordinates and $\mathrm{d}\mathbf{x} = (\mathrm{d}\lambda_1, \mathrm{d}\lambda_2, \mathrm{d}\lambda_3)$ in area co-ordinates (see Figure 2). If the initial scalar profile is given by a known function $\hat{f}$, initial guess for the derivative values is given by $f_j^{(l)} = \partial f/\partial x_l|_{t=0, P_j}$. Otherwise, $f_j^{(l)} = 0$ according to the CIP method [7, 8].

We can estimate the error of the CIVA method by substituting the correct solution $\hat{f}$ with f in Equation (31) and applying the Taylor series analysis (see Appendix A in detail).

$$\begin{aligned}
&\left(\frac{\partial \hat{f}}{\partial t} + u\frac{\partial \hat{f}}{\partial x}\right)\Bigg|_{t^n, P_1} \\
&\quad = (1-2c)\frac{C(1-C)u}{|x_e|}\,\frac{y_2(-y_3)}{(y_2-y_3)^2}\,[|\mathbf{x}_+|^2(\mathbf{e}_+\cdot\nabla)^2\hat{f} + |\mathbf{x}_-|^2(\mathbf{e}_-\cdot\nabla)^2\hat{f}]|_{t^n, P_1} \\
&\qquad + O(\Delta t^2, |\mathbf{x}_2|^2, |\mathbf{x}_3|^2)
\end{aligned} \tag{32}$$

where Courant number is defined by $C = \Delta t|u|/|x_e|$, and

$$\mathbf{x}_+ = \frac{\mathbf{x}_2 + \mathbf{x}_3}{2}, \quad \mathbf{x}_- = \frac{\sqrt{3}(\mathbf{x}_2 - \mathbf{x}_3)}{2}, \quad \mathbf{e}_+ = \frac{\mathbf{x}_+}{|\mathbf{x}_+|}, \quad \mathbf{e}_- = \frac{\mathbf{x}_-}{|\mathbf{x}_-|} \tag{33}$$

x_e is defined as the crossing point between x_1-axis and line of P_2P_3 (Figure 2). The terms $(\mathbf{e}_+\cdot\nabla)^2 f$ and $(\mathbf{e}_-\cdot\nabla)^2 f$, respectively, means the viscosity effect in the direction of $\mathbf{e}_+$ and $\mathbf{e}_-$, and $|\mathbf{x}_+|^2$ and $|\mathbf{x}_-|^2$ represent their respective strength of the effect. From Equation (32), we can make the following important observations.

(a) When $c = 1/2$, the quadratic differential term (first term of the left side) of Equation (32) vanishes and the CIVA method achieves second-order accuracy in both time and space.
(b) When $c < 1/2$, the first term of the left side contributes to the stability of the CIVA method through the numerical or artificial viscosity effect.
(c) The configuration of the triangle determines the directional property of viscosity. When the target triangle is regular ($|\mathbf{x}_+| = |\mathbf{x}_-|$), the artificial viscosity becomes isotropic.
(d) Regarding the term $\{y_2(-y_3)\}/(y_2 - y_3)^2$ with $y_2 \geqslant 0$ and $y_3 \leqslant 0$, the artificial viscosity takes the maximum when $y_2 = -y_3$, namely, the flow is parallel to the bisector direction of $\angle P_2P_1P_3$.
(e) Stable condition of calculation is $0 \leqslant C \leqslant 1$. Thus, the artificial viscosity takes the maximum when $C = 0.5$, that is the flow velocity satisfies $u = |x_e|/(2\Delta t)$.

It is confirmed from (a) that constant curvature conditions assure the second-order accuracy of CIVA in both time and space.

2.4.3. Utilization of another calculation point.
The bubble function can be determined by utilizing information of another point around the vertices of n-simplex. The determination of bubble function for the two-dimensional case is considered here by using the scalar value f_4^n in the point P_4 at t^n shown in Figure 2. While

the inside of triangle is generally an object of area co-ordinates, the co-ordinate values of the point P_4^n can be expressed with area co-ordinates using Equation (4) whose relation also holds in all other region. By using the area co-ordinates of P_4^n; $(\lambda_{4,1}, \lambda_{4,2}, \lambda_{4,3})$, the parameter c' can be calculated from Equation (30) as

$$c' = \left(f_4^n - \sum_{i=1}^{3} \alpha_i \lambda_{4,i} - \sum_{j,k=1(j\neq k)}^{3} \beta_{jk} \lambda_{4,j}^2 \lambda_{4,k} \right) \Big/ \lambda_{4,1}\lambda_{4,2}\lambda_{4,3} \tag{34}$$

From analysis with the Taylor expansion, terms of lower than third order are found to vanish and CIVA with this c' parameter has third-order accuracy in both time and space. This is a generalization of the two-dimensional CIP method that utilizes four calculation points for interpolation.

3. NUMERICAL VERIFICATION

3.1. Two-dimensional problem

The above considerations are verified by numerical experiment with the following two-dimensional advection–diffusion problem:

$$\frac{\partial \hat{f}}{\partial t} + u_i \frac{\partial \hat{f}}{\partial x_i} = \mu \frac{\partial}{\partial x_i} \frac{\partial}{\partial x_i} \hat{f} \tag{35}$$

where μ is the viscosity (diffusion) coefficient. At first, let us describe the strict viscosity model using CIVA. Since $\hat{f}$ in the triangle $\langle P_1P_2P_3 \rangle$ is approximated by a cubic function f, the secondary derivatives of viscosity terms become a linear function. For example, since the secondary partial derivatives of f by x_1 at point P_1 is

$$\begin{aligned} J^2 f_1^{(1,1)} = 2\{ & \beta_{21} x_{3,2}^2 + \beta_{31} x_{2,2}^2 + 2\beta_{13} x_{2,2}(x_{3,2} - x_{2,2}) \\ & - 2\beta_{12} x_{3,2}(x_{3,2} - x_{2,2}) - c' x_{3,2} x_{2,2} \} \end{aligned} \tag{36}$$

where $J = x_{2,1}x_{3,2} - x_{2,2}x_{3,1}$, the profile of secondary derivatives in the triangle is approximated by

$$f^{(1,1)}(\lambda_1, \lambda_2, \lambda_3) = f_1^{(1,1)}\lambda_1 + f_2^{(1,1)}\lambda_2 + f_3^{(1,1)}\lambda_3 \tag{37}$$

If the viscosity terms are evaluated by the upwind method, viscosity at d$\mathbf{x}$ is calculable by

$$\Delta f(\mathrm{d}\lambda_1, \mathrm{d}\lambda_2, \mathrm{d}\lambda_3) = \Delta f_1 \mathrm{d}\lambda_1 + \Delta f_2 \mathrm{d}\lambda_2 + \Delta f_3 \mathrm{d}\lambda_3 \tag{38}$$

where $\Delta f_i = f_i^{(1,1)} + f_i^{(2,2)}$ and so on. The viscosity for the derivative variables can be similarly calculated. Another method to evaluate the viscosity terms was presented in a previous study [6].

Calculating points are collocated in a triangular arrangement as shown in Figure 3. Based on result (32), the numerical viscosity is isotropic in the arrangement, and therefore, the viscosity can be corresponding to the viscosity coefficient of Equation (35). Considered advection–diffusion problem is indicated in Figure 4 where the flow is supposed to be uniform in

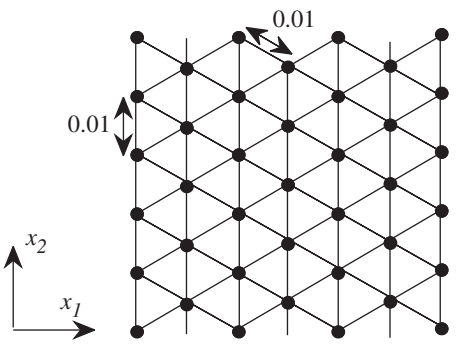

Figure 3. Regular triangular configuration of computing points.

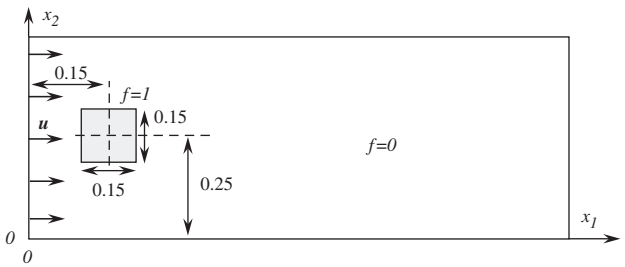

Figure 4. Considered advection–diffusion problem.

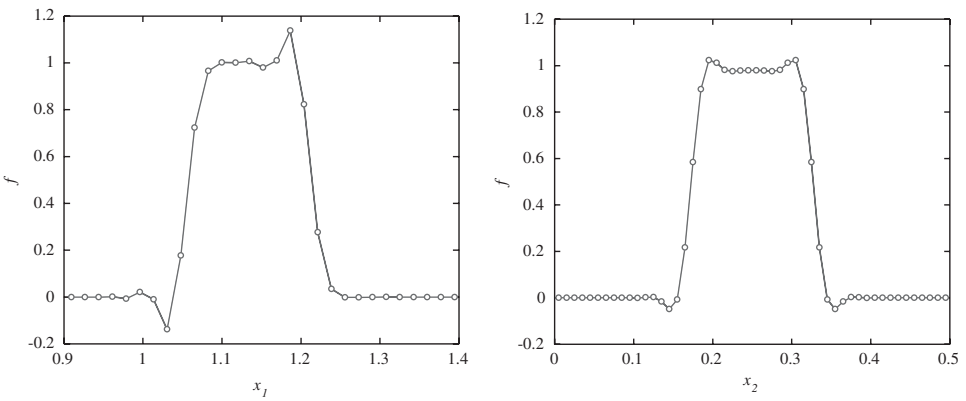

Figure 5. $c = 0.5,\ \mu = 0.0$.

the direction of x_1. The scalar value is profiled by $f=1$ in the region of 0.15×0.15 and $f=0$ in the other region. The calculation is performed in 200 time steps with $\mathbf{u}=(1,0)$ and $\Delta t=0.005(C=1/\sqrt{3})$. At first, the results with no viscosity and $c=0.5$ are shown in Figure 5. The left-side figure is the scalar profile at $x_2=0.25$ and the right-side figure is that at $x_1=1.15$. In this case, since the CIVA method serves as second-order accuracy, some over- and under-

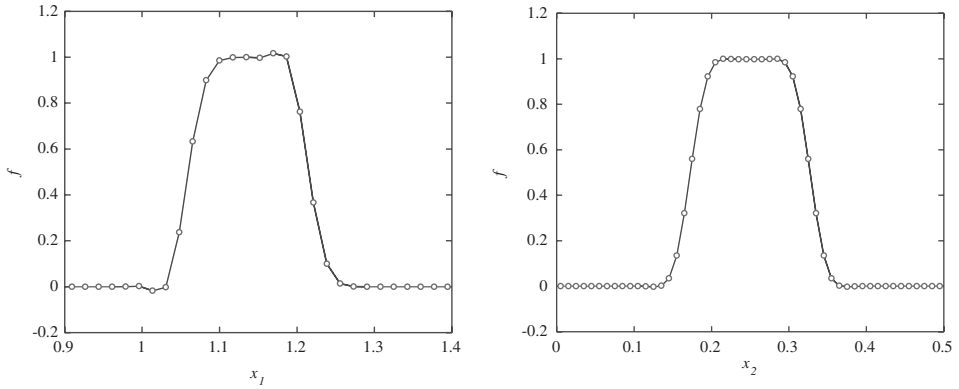

Figure 6. $c = 0.4,\ \mu = 0.0$.

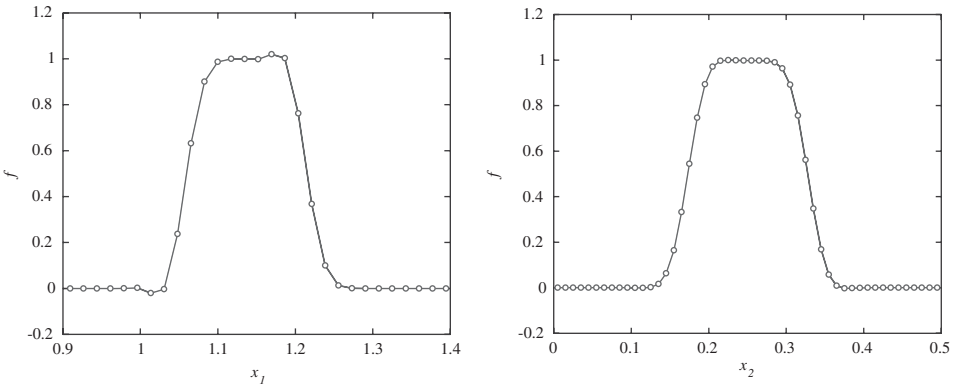

Figure 7. $c = 0.5,\ \mu = 1.06 \times 10^{-4}$.

shootings are confirmed. Next the result with no viscosity and $c=0.4$ are shown in Figure 6. The over- and under-shooting are confirmed to be suppressed by the effect of numerical viscosity. From relation (32), the inviscid advection problem of $c=0.4,\ \mu=0$ is equivalent to the advection–diffusion problem of $c=0.5,\ \mu=1.06\times10^{-4}$ with second-order accuracy (see the appendix). Thus, a calculation using $c=0.5,\ \mu=1.06\times10^{-4}$ was performed, where we use the above-mentioned viscosity model. The result is shown in Figure 7. It agrees well with Figure 6, and the validity of the discussion in Section 2 is supported.

3.2. Filtering techniques to prevent spurious oscillations

In most second- and high-order schemes, the solutions show over- and under-shootings in regions of sharp gradients which can lead to physically unrealistic solutions such as negative mass and energy densities. When the constant curvature condition is used for determining the interpolating functions, the CIVA method has second-order accuracy respecting Taylor expansion. Therefore, the solutions by the CIVA with the constant curvature condition exhibit spurious oscillations near the sharp gradients as is shown in the results of Section 3.1. In

regard to preventing the oscillations, numerical experiments have indicated that a satisfactory filter is to provide an artificial viscosity for the solution. Thus, the control of c-parameter as is shown in the previous section is a simple and effective method for handling the oscillations of solution.

Another popular method for the purpose is to utilize filtering techniques such as FRAM [13] or TVD [14]. The original CIP method is proved to have third-order accuracy both in time and space [6], and thus, the same problems of over- and under-shootings are confirmed in the solutions. To solve the problem, some filtering schemes are introduced into the CIP method [8]. However, the schemes are not applicable to the CIVA method, since they are based on the rectangular mesh system. Thus, we present here a simple filtering method like the FRAM for the CIVA method. In this section, we will consider the two-dimensional case, but the method is easily extended to three dimensions.

We suppose the scalar quantity in a triangle to be the cubic function (13) with the bubble function (18) using $c=1/2$. To avoid the over- and under-shooting, we control the parameter d of the interpolating function by the following algorithms. When time step advances from n to $n+1$, the basic procedures of the FRAM for CIVA can be stated as follows:

(I) Calculate a provisional advanced time solution, $\tilde{f}^{n+1}$, for the system of equations using CIVA (e.g. Evaluation of Equation (31)).

(II) Calculate local bounds on the advanced time solution. In the CIVA-particle method, the Lagrangian update is evaluated by the movement of calculating points according to the flow, that is to say, the scalar values at all the vertices of the target triangle do not change. Thus, the bounds can be obtained by calculating the minimum and maximum values respecting all the vertices of the target triangle at the previous time step,

$$f_{\min}=\min(f_1^n, f_2^n, f_3^n), \quad f_{\max}=\max(f_1^n, f_2^n, f_3^n) \tag{39}$$

(III) Introduce a strong local dissipation flux into the equations when the provisional solution is not within the bounds calculated in step (II) to reduce the overall algorithm to one that is locally monotonic.

In procedure (III), we introduce the local dissipation by switching the interpolating functions properly by the following rules. If the value at a target point in the triangle is in the range, $f_{\min}\leqslant\tilde{f}^{n+1}\leqslant f_{\max}$, we use $d=1$, third-order function, and otherwise, we use $d=0$, linear function. This rule is not a mathematical model but a practical model, because the third-order interpolation function allows the physical values profile in the triangle to exceed the values at vertices, but the filter makes the interpolating function be monotonous. However, if we can use a sufficient number of particles to monotonously approximate the profile, the filter is useful for preventing numerical oscillations. Figure 8 is an example obtained by the filtering technique for the same problem solved in the previous section. The technique works well to prevent spurious oscillations in the case of large gradient.

If the initial data are discontinuous or the velocity field has large gradient, conventional solution procedures become inadequate. In many problems of physical interest large local gradients can occur such as shock flows, shear flows and chemically reacting flows where large gradients in species concentration can occur. In such cases conventional solution procedures can lead to unrealistic results.

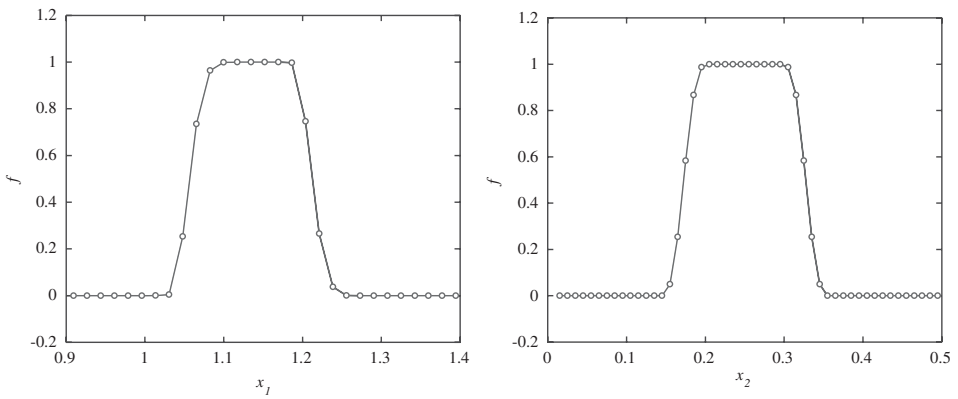

Figure 8. The results obtained with filtered CIVA.

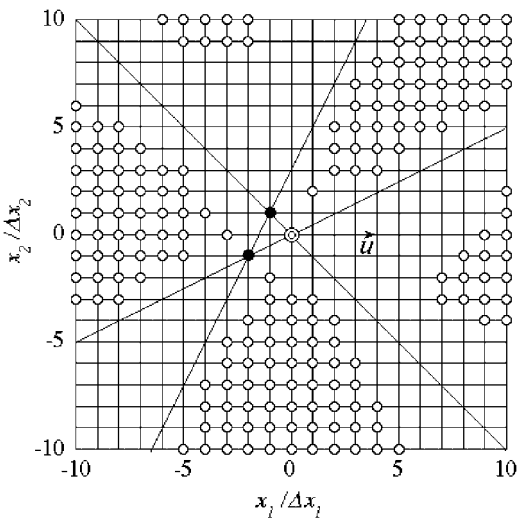

Figure 9. Stability map obtained by numerical calculation (mesh points were the checked points and the circle means that the calculation was stable at the point).

3.3. Utilization of another point data

For the approach using the fourth point, the same problem as the above was analysed using the calculation point arranged in rectangular mesh. Viscosity was set to 0. As is shown in Figure 9, when the co-ordinates of the considered point (double circle) are supposed to be $(0,0)$, the triangle used for interpolation is constructed with the filled-circle points whose relative positions are $(-1,1)$ and $(-2,-1)$. Stability of calculation was checked by changing the fourth point position. The stability map about the position of the fourth point relative to the considered point is shown in Figure 9. The blank circle means a position with which the calculation was stably performed and the other lattice point means a position

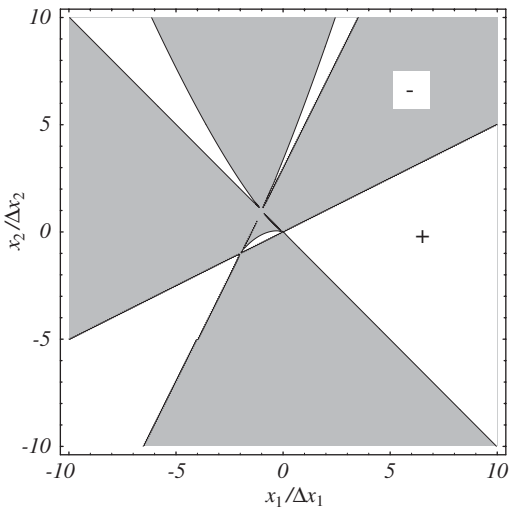

Figure 10. Stability map based on sign of coefficient of $f^{(1,1,1,1)}$ by analytical calculation (hatched area was evaluated to be stable).

with which the calculation was unstable. The calculation becomes unstable near the straight lines composing triangle edges because the denominator $\lambda_{4,1}\lambda_{4,2}\lambda_{4,3}$ in Equation (34) is close to 0. However, in the case that the considered triangle and the fourth point construct a parallelogram, the solution is stably obtained in spite of the point neighbouring the straight lines composing triangle edges. For the moment, the reason for this is unknown. As mentioned above, respecting Taylor expansion, since this approach has third-order accuracy in time and space, the fourth derivatives are deemed to affect stability of the solution. Therefore, the sign of the coefficient of $f^{(1,1,1,1)}$, which is regarded as having the strongest influence among the fourth-order derivatives, was investigated (Appendix B). The analytical result is shown in Figure 10. As the condition for stability is the sign of the fourth derivative being negative, we consider that the results explain fairly well the stability shown in Figure 9. Moreover, although the stable point appears in the unstable domain at the point separated far from the triangle, this is considered to be because the domain is where the distance to P_4 compared with the representing distance of the triangle is too long to hold the Taylor expansion approximation.

3.4. Three-dimensional passive scalar advection problem

While the derivation is too complicated to be shown here, we can prove by the same approach as in the appendix that the constant curvature conditions in three dimensions also assure the second-order accuracy of CIVA in both time and space. Some computational results using the three-dimensional function (27) are described in Reference [15]. From the results, we can confirm that the CIVA method with constant curvature conditions has an accuracy between that of third-order upwind scheme and that of fourth-order central difference scheme. This fact also support our consideration based on the Taylor series analysis.

4. CONCLUSION

The accuracy and stability of a highly accurate interpolation method, CIVA, was evaluated by mathematical and numerical analyses. First, the general formulation of CIVA for the n-dimensional case was described. Then, two determination methods for bubble function of CIVA, constant curvature condition and utilization of another computing point, was considered. The bubble function in the CIVA method was analysed based on the Taylor expansion, and was found to play a role of adding artificial viscosity to the solution. Some computations of two-dimensional passive scalar advection and advection–diffusion problems were performed for the verification of accuracy and stability. From the results, both the bubble function and the filtering technique were also found to be effective in order to control over- and under-shootings of CIVA.

APPENDIX A: ESTIMATION OF TRANCATION ERROR BASED ON TAYLOR SERIES ANALYSIS

In this appendix, we derive Equation (32) from the Taylor series analysis of the CIVA-based advection solvers. Since only a two-dimensional problem is considered in this section, we use $x=x_1, y=x_2, f^x=f^{(1)}$ and $f^y=f^{(2)}$ for simplicity. Two-dimensional uniform flow is supposed to be in the direction of x, $\mathbf{u}=(u,0)$ (see Figure 2). Under the conditions, both the CIVA-particle and CIVA-gridless methods evaluate the value at the position P_1 and the time $t=t^{n+1}$ by

$$\begin{aligned} f_1^{n+1} &= f^n(\mathrm{d}\lambda_1, \mathrm{d}\lambda_2, \mathrm{d}\lambda_2) \\ &= \sum_{i=1}^{3} \alpha_i \mathrm{d}\lambda_i + \sum_{j,k=1(j\neq k)}^{3} \beta_{jk}(\mathrm{d}\lambda_j^2 \mathrm{d}\lambda_k + c\,\mathrm{d}\lambda_1 \mathrm{d}\lambda_2 \mathrm{d}\lambda_3) \end{aligned} \tag{A1}$$

$$\alpha_i = f_i^n, \quad \beta_{jk} = f_j^n - f_k^n + (x_k - x_j) f_j^{x,n} + (y_k - y_j) f_j^{y,n} \tag{A2}$$

The area co-ordinates $(\mathrm{d}\lambda_1, \mathrm{d}\lambda_2, \mathrm{d}\lambda_3)$ can be calculated by Equation (4), that is

$$\begin{pmatrix} \mathrm{d}\lambda_1 \\ \mathrm{d}\lambda_2 \\ \mathrm{d}\lambda_3 \end{pmatrix} = \begin{pmatrix} 0 & x_2 & x_3 \\ 0 & y_2 & y_3 \\ 1 & 1 & 1 \end{pmatrix}^{-1} \begin{pmatrix} -\Delta tu \\ 0 \\ 1 \end{pmatrix} \tag{A3}$$

Here, we substitute the strict solution $\hat{f}$ with f in Equation (A1) and estimate the error of the CIVA method. The two-dimensional Taylor expansions for $\hat{f}_2^n, \hat{f}_3^n, \hat{f}_2^{x,n}, \hat{f}_2^{y,n}, \hat{f}_3^{x,n}, \hat{f}_3^{y,n}$ around the point P_1 and the time t^n are carried out. For example,

$$\hat{f}_2^n = \hat{f}_1^n + (\mathbf{x}_2 \cdot \nabla)\hat{f}|_{t^n,P_1} + \frac{1}{2}(\mathbf{x}_2 \cdot \nabla)^2 \hat{f}|_{t^n,P_1} + O_1(|\mathbf{x}_2|^3) \tag{A4}$$

$$\hat{f}_2^{x,n} = \hat{f}_1^{x,n} + (\mathbf{x}_2 \cdot \nabla)\hat{f}^x|_{t^n,P_1} + O_2(|\mathbf{x}_2|^2) \tag{A5}$$

$$\hat{f}_3^{x,n} = \hat{f}_1^{x,n} + (\mathbf{x}_3 \cdot \nabla)\hat{f}^x|_{t^n,P_1} + O_3(|\mathbf{x}_3|^2) \tag{A6}$$

Substituting all these results for f in RHS of Equation (A1) leads to

$$\begin{aligned}(\mathrm{RHS}) = \hat{f}_1^n - \Delta t u \hat{f}_1^{x,n} + \Delta t^2 \frac{u^2}{2} \hat{f}_1^{xx,n} \\ + (1-2c)\frac{\Delta t^2 u^2 y_2(-y_3)}{J^2}\left[1 - \frac{\Delta t u(y_3 - y_2)}{J}\right](s_1 \hat{f}_1^{xx,n} + s_2 \hat{f}_1^{xy,n} + s_3 \hat{f}_1^{yy,n}) \\ + O(|\mathbf{x}_2|^3, |\mathbf{x}_3|^3) \end{aligned} \tag{A7}$$

where

$$J = x_2 y_3 - y_2 x_3, s_1 = x_2^2 + x_3^2 - x_2 x_3, s_2 = 2x_2 y_2 + 2x_3 y_3 - x_2 y_3 - x_3 y_2, s_3 = y_2^2 + y_3^2 - y_2 y_3 \tag{A8}$$

By means of vectors (33), we can rewrite

$$s_1 \hat{f}_1^{xx,n} + s_2 \hat{f}_1^{xy,n} + s_3 \hat{f}_1^{yy,n} = [|\mathbf{x}_+|^2 (\mathbf{e}_+ \cdot \nabla)^2 \hat{f} + |\mathbf{x}_-|^2 (\mathbf{e}_- \cdot \nabla)^2 \hat{f}]|_{t^n, P_1} \tag{A9}$$

Let us introduce new quantities defined by the following equations:

$$x_e = -\frac{J}{y_2 - y_3}, \quad C = \frac{\Delta t u}{|x_e|} \tag{A10}$$

x_e is defined as the crossing point between x-axis and segment P_2P_3 (see Figure 2) and C is the Courant number. By using the quantities, the following relations are established:

$$\frac{\Delta t^2 u^2 y_2(-y_3)}{J^2}\left[1 - \frac{\Delta t u(y_3 - y_2)}{J}\right] = \Delta t \frac{C(1-C)u}{|x_e|} \frac{y_2(-y_3)}{(y_2 - y_3)^2} \tag{A11}$$

On the other hand, Taylor expansion for $\hat{f}_1^{n+1} = \hat{f}_1(t^n + \Delta t)$ around the point P_1 and the time t^n is

$$\hat{f}_1^{n+1} = \hat{f}_1^n + \Delta t \left.\frac{\partial \hat{f}}{\partial t}\right|_{t^n, P_1} + \frac{\Delta t^2}{2} \left.\frac{\partial^2 \hat{f}}{\partial t^2}\right|_{t^n, P_1} + O_4(\Delta t^3) \tag{A12}$$

By substituting this result for f^{n+1} in Equation (A1), we can obtain

$$\begin{aligned}\left.\left(\frac{\partial \hat{f}}{\partial t} + u\frac{\partial \hat{f}}{\partial x}\right)\right|_{t^n, P_1} = \Delta t \frac{u^2}{2} \hat{f}_1^{xx,n} - \frac{\Delta t}{2} \left.\frac{\partial^2 \hat{f}}{\partial t^2}\right|_{t^n, P_1} + (1-2c)\frac{C(1-C)u}{|x_e|} \frac{y_2(-y_3)}{(y_2 - y_3)^2} \\ \times [|\mathbf{x}_+|^2 (\mathbf{e}_+ \cdot \nabla)^2 \hat{f} + |\mathbf{x}_-|^2 (\mathbf{e}_- \cdot \nabla)^2 \hat{f}]|_{t^n, P_1} \\ + O(\Delta t^2, |\mathbf{x}_2|^2, |\mathbf{x}_3|^2) \end{aligned} \tag{A13}$$

Since the flow is uniform, $\mathbf{u} = (u, 0)$, the governing equation (28) causes the relations

$$\left.\frac{\partial^2 \hat{f}}{\partial t^2}\right|_{t^n, P_1} = -u \left.\frac{\partial}{\partial t}\frac{\partial \hat{f}}{\partial x}\right|_{t^n, P_1} = u^2 \left.\frac{\partial^2 \hat{f}}{\partial x^2}\right|_{t^n, P_1} = u^2 \hat{f}_1^{xx,n} \tag{A14}$$

By utilizing the relations, Equation (A13) is transformed to

$$\left(\frac{\partial \hat{f}}{\partial t}+u\frac{\partial \hat{f}}{\partial x}\right)\Bigg|_{t^n,P_1}$$
$$=(1-2c)\frac{C(1-C)u}{|x_e|}\frac{y_2(-y_3)}{(y_2-y_3)^2}[|\mathbf{x}_+|^2(\mathbf{e}_+\cdot\nabla)^2\hat{f}+|\mathbf{x}_-|^2(\mathbf{e}_-\cdot\nabla)^2\hat{f}]|_{t^n,P_1}$$
$$+O(\Delta t^2,|\mathbf{x}_2|^2,|\mathbf{x}_3|^2) \tag{A15}$$

Example (*the same problem as Section 3.2*): When $P_1P_2P_3$ is a regular triangle with length r on a side and the flow is parallel to the bisector direction of $\angle P_2P_1P_3$,

$$\mathbf{e}_+\perp\mathbf{e}_-,\quad |\mathbf{x}_+|=|\mathbf{x}_-|=|x_e|=\frac{\sqrt{3}r}{2} \tag{A16}$$

Thus, Equation (A15) becomes

$$\left(\frac{\partial \hat{f}}{\partial t}+u\frac{\partial \hat{f}}{\partial x}\right)\Bigg|_{t^n,P_1}=\mu_a\left(\frac{\partial^2}{\partial x^2}+\frac{\partial^2}{\partial y^2}\right)\hat{f}\Bigg|_{t^n,P_1}+O(\Delta t^3,r^3) \tag{A17}$$

where the artificial viscosity coefficient μ_a becomes

$$\mu_a=(1-2c)C(1-C)\frac{\sqrt{3}ur}{8} \tag{A18}$$

Therefore, under the same condition as that in Section 3.2 ($u=1, r=0.01, C=1/\sqrt{3}$), the inviscid advection problem of $c=0.4$ and $\mu=0$ is equivalent to the advection–diffusion problem of $c=0.5$ and $\mu_a=1.0566\times10^{-4}$ with second-order accuracy.

APPENDIX B: COEFFICIENT OF $\hat{f}^{(1,1,1,1)}$ WHEN UTILIZING ANOTHER POINT DATA

In the case considered in Section 3.3, the Taylor series analysis leads to the following estimation:

$$\left(\frac{\partial \hat{f}}{\partial t}+u\frac{\partial \hat{f}}{\partial x}\right)\Bigg|_{t^n,P_1}=\eta_a\hat{f}^{(1,1,1,1)}|_{t^n,P_1}+\text{other fourth-order derivative terms} \tag{B1}$$

where

$$\eta_a=-\frac{d_1\Delta t+d_2\Delta t^2}{216(x_4-2y_4)(3+2x_4-y_4)(x_4+y_4)}-\frac{\Delta t^3}{24}$$
$$d_1=-40x_4^2-27x_4^3-135x_4y_4-111x_4^2y_4-162y_4^2-75x_4y_4^2+50y_4^3$$
$$d_2=-40x_4^2+18x_4^3+130x_4y_4+114x_4^2y_4+188y_4^2+90x_4y_4^2-60y_4^3$$

REFERENCES

1. Harlow FH. The particle-in-cell method for fluid dynamics. In *Methods in Computer Physics*. Alder B, Fernbach S, Rotenberg M (eds.), vol. 3. Academic Press: New York. 1964; 319.
2. Batina JT. A gridless Euler/Navier–Stokes solution algorithm for complex-aircraft applications. *AIAA Paper 93-0333*, 1993.
3. Monaghan JJ. An introduction to SPH. *Computer Physics Communications* 1988; **48**:89–96.
4. Liu WK, Sihling DT, Chen Y, Hao W. Multiresolution reproducing kernel particle methods for computational fluid dynamics. *International Journal for Numerical Methods in Fluids* 1997; **24**:1391–1415.
5. Sukumar N, Moran B, Belytschko T. Natural element method in solid mechanics. *International Journal for Numerical Methods in Engineering* 1998; **43**:839–887.
6. Tanaka N. Development of highly accurate interpolation method for mesh-free flow simulations I. Integration of gridless, particle and CIP methods. *International Journal for Numerical Methods in Fluids* 1999; **30**:957–976.
7. Yabe T, Aoki T. A universal solver for hyperbolic equations by cubic-polynomial interpolation I. One-dimensional solver. *Computer Physics Communications* 1991; **66**:219–232.
8. Yabe T, Ishikawa T, Wang PY. A universal solver for hyperbolic equations by cubic-polynomial interpolation II. Two- and three-dimensional solvers. *Computer Physics Communications* 1991; **66**:233–242.
9. Pierre R. Simple C^0 approximations for the computation of incompressible flows. *Computer Methods in Applied Mechanics and Engineering* 1988; **68**:205–227.
10. Brezzi F, Bristeuu MO, Franca LP, Mallet M, Roge G. A relationship between stabilized finite element methods and the Galerkin method with bubble functions. *Computer Methods in Applied Mechanics and Engineering* 1992; **96**:117–129.
11. Zienkiewicz OC. *The Finite Element Method* (3rd edn). McGraw-Hill: New York, 1977.
12. Bazeley GP, Cheung YK, Irons BM, Zienkiewicz OC. The triangular elements in bending-conforming and non-conforming solutions. *Proceedings of the Conference on Matrix Methods in Structural Mechanics*. Air Force Institute of Technology: Wright Patterson A.F. Base, OH, 1965.
13. Chapman M. FRAM—nonlinear damping algorithms for the continuity equation. *Journal of Computer Physics* 1981; **44**:84–103.
14. Harten A. High resolution scheme for hyperbolic conservation laws. *Journal of Computer Physics* 1981; **49**:357.
15. Tanaka N. Development of highly accurate interpolation method for mesh-free flow simulations II. Application of CIVA to incompressible fluid simulations. *International Journal for Numerical Methods in Fluids* 2000; **34**:403–424.

